

# Recovery and Separation of Carbohydrate Derivatives from the Lipid Extracted Alga *Dunaliella* by Mild Liquefaction

Liisa K. Rihko-Struckmann,<sup>\*,†</sup> Mark Molnar,<sup>†</sup> Kristin Pirwitz,<sup>†</sup> Melanie Facht,<sup>†</sup> Kevin McBride,<sup>†</sup> Alexander Zinser,<sup>†</sup> and Kai Sundmacher<sup>†,‡</sup>

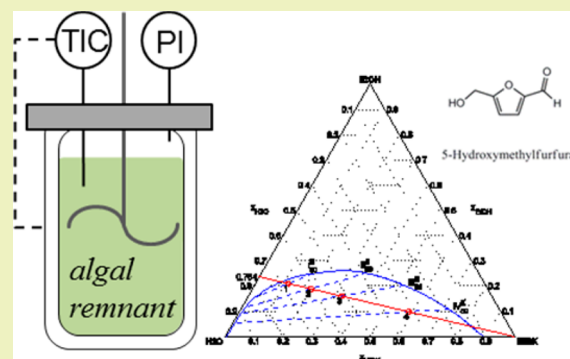
<sup>†</sup>Max Planck Institute for Dynamics of Complex Technical Systems, D-39106 Magdeburg, Germany

<sup>‡</sup>Otto-von-Guericke University Magdeburg, Universitätsplatz 2, D-39106 Magdeburg, Germany

## Supporting Information

**ABSTRACT:** The main product obtained in the industrial cultivation of green microalgae *Dunaliella salina* is natural  $\beta$ -carotene. After the extraction of the valuable pigment an algae residue remains. This remnant was hydrolyzed under mild liquefaction conditions at 453 K for 1 h in various ethanol/water ratios. A heterogeneous acidic catalyst, Nafion NR50, was used in one experiment for comparison. The main compounds comprising the soluble fraction were identified. Methyl isobutyl ketone (MIBK) was used as extraction solvent to obtain 5-hydroxymethylfurfural (5-HMF) as a product. The 5-HMF solubility in the ternary ethanol/water/MIBK mixtures along the binodal curve was predicted by the quantum chemical method COSMO-RS. The partition of the 5-HMF in the MIBK rich extract and the aqueous phase was estimated based on the prediction. Theoretically, 96.2% of 5-HMF can be recovered in the MIBK rich extract in liquefaction conditions with an ethanol/water ratio of 50/50 (v/v). Experimentally, 10.3 mg of 5-HMF per gram of the remnant (dw) was recovered in the organic MIBK phase.

**KEYWORDS:** Liquefaction, *Dunaliella salina*, Lipid extracted algae, Remnant, 5-Hydroxy methyl furfural



## INTRODUCTION

*D. salina* is an algal species that can grow under high salinity.<sup>1</sup> The alga accumulates high amounts of  $\beta$ -carotene and glycerol in response to nitrogen deprivation and abiotic light stress. *D. salina* marine alga is industrially cultivated in open ponds to produce natural  $\beta$ -carotene. The hexane extraction of the lipophilic fraction is the most common industrial method to obtain the valuable pigment today.<sup>2</sup> After the extraction, a defatted algae residue remains. The exploitation of this remnant fraction has become an active research topic recently, because it is seen as being one of the key factors for improving the profitability of the algal industry and for achieving a net positive energy balance.<sup>3–5</sup>

Hydrothermal liquefaction (HTL) is an established thermochemical treatment method for the raw (nonextracted) algal biomass. As is common in HTL, the algal biomass is treated at elevated temperatures from 473 to 673 K and high pressures using water as the reaction medium in order to produce a liquid biocrude soluble in organic solvents (e.g. dichloromethane or hexane).<sup>6</sup> The influence of the HTL conditions, catalysts, solvent mixtures, and the operating mode on the yield and biocrude properties was intensively investigated in lab and pilot scale,<sup>7,8</sup> and even the large scale production issues have been addressed.<sup>9</sup> The desired final product of the conventional HTL is a fuel. To fulfill the specifications required for a fuel, further

defunctionalization, such as hydrodeoxygenation, is necessary for the biocrude.<sup>4,10,11</sup>

Another option for capitalizing on the remnant biomass is by using a mild hydrothermal treatment with the goal of decomposing the algal carbohydrates and proteins. The mild reactor conditions (temperature < 473 K, autonomous pressure) preferably facilitate the hydrolysis of the biomacromolecules to soluble monomers and their derivatives. In contrast to the conventional HTL this approach does not produce a biocrude suitable as a fuel but sugars and other highly valuable functionalized chemical compounds. The bacterium *Z. mobilis* converted the hydrolysate of the microalgae *C. vulgaris* to ethanol.<sup>12</sup> The aqueous phase solubles (mainly glucose) obtained in the mild hydrolysis of *D. salina* remnant was used as a carbon source in the cultivation of *C. vulgaris*, *E. coli*, and *S. cerevisiae*.<sup>13</sup> The processing of microalgal biomass with the aim of producing renewable chemical compounds has been addressed by very few groups so far.<sup>14</sup>

The most common reaction medium used in the HTL for algal biomass is water. Water is a preferable solvent for many reasons including its low cost and its beneficial effects as a solvent on the reaction when operated close to or above

Received: August 16, 2016

Revised: November 23, 2016

Published: November 25, 2016

supercritical conditions (>647 K and 22.1 MPa). Recently, the effects of other media and the use of binary solvent mixtures on liquefaction have been studied with the goal of increasing the conversion.<sup>15–19</sup> Yuan et al. reported that methanol as a solvent resulted in the highest decomposition conversion in *Spirulina* liquefaction compared to ethanol and 1,4-dioxane.<sup>16</sup> The use of alcohols as cosolvents in aqueous reaction media increases the bio-oil yield, facilitates the conversion, and suppresses the formation of solid residuals. Alcohols react preferably with acidic components to form esters, prevent coking by dissolving large molecules, and stabilize free radicals thus reducing polymerization due to their ability to donate protons.<sup>17–19</sup> The best biocrude yield from *Chlorella pyrenoidosa* was obtained by applying a water–ethanol cosolvent mixture.<sup>19</sup> The inclusion of ethanol lowers the dielectric constant and the critical values compared to those of pure water. This positive effect of ethanol as cosolvent was reported for the liquefaction of oleaginous yeast.<sup>20</sup>

The present paper reports the results from our investigation using ethanol in the mild thermal treatment of the lipid-extracted alga *D. salina*. The main intention was to explore, identify, and recover the functionalized chemical compounds formed from the algal remnant. Computational methods were used to estimate the solubility of one identified compound, 5-hydroxymethylfurfural (5-HMF), showing the proof-of-principle for possible separation and recovery.

### SOLUBILITY ESTIMATION BY COSMO-RS

Today, computational chemistry has become a pertinent tool for process design. It allows one to predict thermodynamic properties in the absence of empirical data or model specific molecular parameters. One such method is the *ab initio* Conductor like Screening Model for Real Solvents (COSMO-RS).<sup>21</sup> This model uses quantum chemically generated surface charge densities of the molecules and can satisfactorily predict several thermodynamic properties of pure liquids or liquid mixtures based on the molecular surface interactions. This is especially useful in estimating compound solubilities in solvent mixtures where little or no data is available.

The COSMO-RS theory has been successfully used for predicting the thermodynamic properties of key products and intermediates from biomass<sup>22</sup> or the solubilities of pharmaceuticals in solvent screening.<sup>23</sup> Recently, the method was satisfyingly applied in the solubility estimation of a homogeneous catalyst–ligand system in order to design a thermomorphic solvent system.<sup>24</sup> In the present work, the goal is to estimate the solubility in a solvent mixture that extracts the identified compound, 5-HMF, from the algal biomass. Ternary solvent mixtures consisting of methyl isobutyl ketone (MIBK), ethanol (EtOH), and water (H<sub>2</sub>O) are considered. The solubility of 5-HMF is predicted for solvent compositions taken from liquid–liquid equilibria of MIBK–EtOH–H<sub>2</sub>O. COSMO-RS is implemented using the software COSMOtherm with the extended database COSMObase using the BP-TZVPD-FINE-C30-1501 parametrization.<sup>25</sup>

### MATERIALS AND METHODS

**Materials.** *Dunaliella salina* powder provided by Monzón Biotech S.L., Spain, was used for the liquefaction experiments. The powder was initially extracted with hexane (quality >99%, Sigma-Aldrich) in a lab scale Soxhlet extractor (100 mL) to simulate the industrial product recovery of the lipophilic, high-value ingredient,  $\beta$ -carotene. A batch of 12 g of the fresh powder was placed on filter paper ( $d = 185$  mm, pore

size = 7–12  $\mu\text{m}$ ) and extracted with 200 g of hexane for 5 h. The remnant alga was dried at room temperature for 12 h. The water content was determined by heating a  $\sim 0.5$  g sample in a porcelain crucible at 343 K for 12 h. The ash content was determined by heating  $\sim 0.5$  g of dried biomass in a furnace at 723 K for 12 h assuming the residue to be nonvolatile ash. The carbon, hydrogen, and nitrogen contents of extracted biomass were determined with a CHN analyzer by Currenta GmbH, Leverkusen, Germany. The oxygen content of the extracted biomass was calculated by subtraction from the content of C, H, N, and ash (see Table 1). The residual lipid content of the remnant

**Table 1. Composition of *D. salina* Remnant after Hexane Extraction<sup>d</sup>**

content [wt %]	
water (initial) [W]	5.6
ash (450 °C) [A]	6.3
lipid [L] <sup>a</sup>	6.8
protein [P]	7.1
carbohydrate [CH] <sup>b</sup>	74.2
elemental composition [wt %], (dw)	
C	40.7
H	7.0
N	1.6
O <sup>c</sup>	50.7

<sup>a</sup>Before extraction 9.1 wt %. <sup>b</sup>[CH] = 100 - [L] - [P] - [A] - [W]. <sup>c</sup>[O] = 100 - [C] - [H] - [N] - [Ash]. <sup>d</sup>Water content refers to the initial value (as delivered) before extraction.

sample was determined with a modified method originating from Blich and Dyer.<sup>26</sup> The protein content (P) was estimated from the content of nitrogen by eq 1:<sup>27</sup>

$$[\text{P}/\text{wt} \ %] = 4.4401 \times [\text{N}/\text{wt} \ %] \quad (1)$$

Table 1 lists the water and ash content and the elemental and the organic macromolecule composition of the remnant.

**Liquefaction.** For the liquefaction, a batch (6 g) of extracted algal biomass and 100 mL of solvent (water, ethanol, or ethanol/water mixtures) was placed into an autoclave reactor (Picoclave3, 200 mL, Buechi, Switzerland). The experiments were carried out with the liquefaction medium having ethanol/water (E/W) ratios of 0/100, 25/75, 50/50, 75/25, and 100/0 (v/v). One experiment (E/W 100/0) was catalyzed with acidic catalyst by loading 1 g of Nafion (NRS0, Ion Power Inc., spherical granules with average diameter of 2–3 mm, CAS 31175-20-9) into a catalyst basket within the autoclave. After loading, the reactor was purged with N<sub>2</sub> gas for 10 min to create an inert atmosphere and heated up to 453 K. The liquefaction suspension was mixed at 2000 rpm with a Buechi Glas Uster cyclone 075 stirrer, and the reactor was kept at 453 K for 60 min during all experiments. The autoclave pressure was recorded but not regulated. The autonomous pressure varied between 10 and 20 bar depending on the applied E/W ratio. This confirmed that a negligible amount of decarboxylation or other decomposition gases was formed. After the desired reaction time (60 min) at 453 K the reactor was cooled to room temperature, and the gases were vented. The experiment with the E/W ratio of 100/0 (v/v) was repeated three times to confirm the reproducibility and the standard deviation of the yields.

**Solid Conversion and Separation of the Products.** After each experiment the reactor suspension was carefully filtered to separate the unconverted solid particles using filter paper (diameter = 185 mm, pore size = 7–12  $\mu\text{m}$ , Whatman). The solid particles were further extracted using acetone for 1 h in a Soxhlet extractor and dried at 343 K for 12 h to quantify the dry weight of the residue. The conversion to solubles, X, in the liquefaction experiment was calculated according to eq 2

$$X = \frac{m_{\text{BM,dw}} - m_{\text{RES,dw}}}{m_{\text{BM,dw}}} \quad (2)$$

where  $m_{\text{BM,dw}}$  is the mass of the algal biomass (dw) loaded into the reactor, and  $m_{\text{RES,dw}}$  is the mass (dw) of the remaining solid residue measured after the liquefaction and acetone extraction.

Methyl isobutyl ketone (MIBK, 4-methyl 2-pentanone, quality >99.5%, Sigma-Aldrich) was used to divide the postreaction mixture into two phases – an aqueous phase and a MIBK-rich phase. MIBK is known as being a good solvent for 5-HMF, and the liquid–liquid–equilibria (LLE) of the ethanol–water–MIBK ternary system was recently published.<sup>28</sup>

#### Analysis of the Reaction Mixture and the MIBK Rich Phase.

Liquid samples (~1.2 mL) were taken both directly from the reaction effluent after solid separation and the MIBK rich phase after phase separation. The samples were analyzed in a gas chromatography GC/MS, Agilent 6890N gas chromatograph with an HP5-column (30 m, diameter 0.32 mm, film 0.25  $\mu\text{m}$ ) under the following conditions: helium carrier gas: 1 mL/min; injector: split mode (1:10), 523 K, 2 bar (overpressure); column temperature: from 398 K with a rate of 8 K/min to 418 K (26 min holding time) and then raised with a rate of 2 K/min to 493 K (10 min holding time). The compounds were identified using NIST MS Search 2.0 database.

**Quantification of 5-HMF.** One valuable product detected in our experiments was 5-HMF. The calibration equation was defined with solutions of 5-HMF ( $\geq 99\%$ , Sigma-Aldrich) which were analyzed by the GC/MS. The amount of 5-HMF in the samples [mg 5-HMF/g solution] was quantified with the calibration equation.

In the following discussion  $I_i$  to  $IV_j^i$  give the ternary compositions as follows:  $i$  refers to the applied E/W (ethanol/water) ratio, i.e.  $i = 50$  for E/W 50/50 (v/v) and  $i = 25$  for E/W 25/75 (v/v). The superscript  $j = E$  refers to MIBK rich phase,  $j = A$  for aqueous phase, and  $j = M$  to the overall composition. The points  $I_i^j$  to  $IV_j^i$  refer to four compositions containing various amount of MIBK.

## RESULTS AND DISCUSSION

**Solid Conversion.** All liquefaction experiments were conducted at 453 K using pure water, ethanol (E/W ratio 100/0), or ethanol/water mixtures having E/W ratios of 25/75, 50/50, and 75/25 (v/v) as reaction medium.

The conversion of the algal biomass to solubles,  $X$ , as a function of the applied E/W ratio is illustrated in Figure 1. The

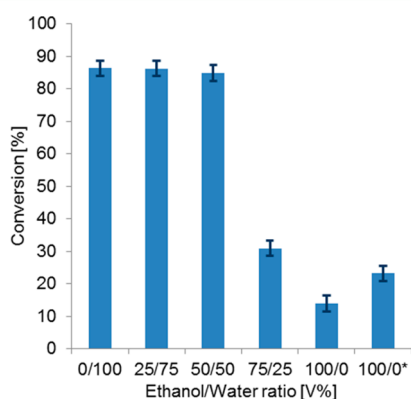


**Figure 1.** Conversion (w/w, eq 2) of the solid algal biomass by mild liquefaction as a function of the ethanol/water ratio (v/v,  $T = 453$  K,  $p = 10$  to 20 bar depending on the E/W ratio). The bar lines show the standard deviation. The experiment 100/0\* was catalyzed by Nafion NRS0.

conversion was high (approximately 86–88%) in experiments with the E/W ratios of 0/100, 25/75, and 50/50 (v/v) without a distinct difference between these experiments. In the experiments applying the E/W ratios of 75/25 and 100/0 (v/v) the biomass conversion to solubles was clearly lower, being only 31% and 14%, respectively. Pure water would be a good

liquefaction medium for the remnant of *D. salina*, but pure ethanol does not facilitate the liquefaction to the same extent. Our findings are in agreement with the results reported by Peng et al.<sup>29</sup> They observed that the addition to ethanol contributed positively to the decomposition of the solid residues. They suggested that ethanol provides an active hydrogen and breaks large molecules into small ones under conventional hydro-treating conditions. However, they reported as well that at ethanol content above 60% facilitated the solid residue repolymerization and the morphology changed to compact and blocky structure. For comparison, the ethanol/water mixture activity was predicted also computationally. Qualitatively, COSMO-RS predicted the lowering solubility as a function of the increasing E/W ratio using glucose as the model solute compound. Based on the obtained experimental results we conclude that algal biomass conversion to soluble substances is strongly dependent on the E/W composition. It is well-known that the decomposition of carbohydrates, e.g. cellulose or fructose, is supported by acidic or bifunctional catalysts.<sup>30,31</sup> However, in most of the experiments presented here no catalyst was used, and released acidic compounds likely catalyze the reactions.

For comparison, one liquefaction experiment (E/W = 100/0) was conducted with the heterogeneous acidic catalyst, Nafion NR-50 (see Figure 1). This catalyst is a perfluorinated sulfonic acid copolymer which tolerates higher reaction temperatures (melting point 473 K) than conventional ion exchange resins (melting point 393 K). In the experiment with pure ethanol, the presence of the Nafion catalyst facilitated the solid conversion to solubles, increasing the conversion from 14% (nuncatalyzed) to 23% as shown in Figure 1. When applying E/W ratios of 25/75, 50/50, and 75/25 (v/v) the catalyst could not be used due to its partial dissolution in the mixture. This was evident after a viscous, nonfilterable reaction effluent was received in one preliminary experiment using an E/W ratio of 75/25 in the presence of the catalyst.

The *D. salina* remnant contains a low amount of proteins. This is due to the severe stress conditions resulting from nitrogen deprivation necessary for inducing the  $\beta$ -carotene synthesis. This was also confirmed by the low nitrogen content of the algal biomass (elemental analysis in Table 1) after lipid extraction. The nonpolar compounds, especially the  $C_{40}$  tetraterpenoid  $\beta$ -carotene, were extracted into the hexane phase. Thus, the remnant biomass contained mainly carbohydrates. Based on our results we conclude that the carbohydrates in the *D. salina* remnant are easily accessible and prone to hydrolysis due to the fragile cell wall of *D. salina*. The carbohydrates are hydrolyzed forming monosaccharides, e.g. glucose, or to sugar dehydration products which are soluble under the applied mild liquefaction conditions, explaining the high biomass conversion.

**Analysis of the Solubles.** After filtration and separation of the solid particles, samples of the reactor effluent were directly analyzed by GC/MS. The chromatograms with the identification of main product peaks for various E/W ratios are shown in Figure 2. The ethanol had a retention time (RT) of 3.75 min and is truncated in the illustration. The liquid product compounds were identified based on the MS signal by the NIST MS Database. The Area-% for the main compounds in the graphs in Figure 2 are given numerically in the Supporting Information (Table S1). Due to the limited tolerance of the MS detector for aqueous samples, the sample with pure water was excluded from the direct GC/MS analysis.

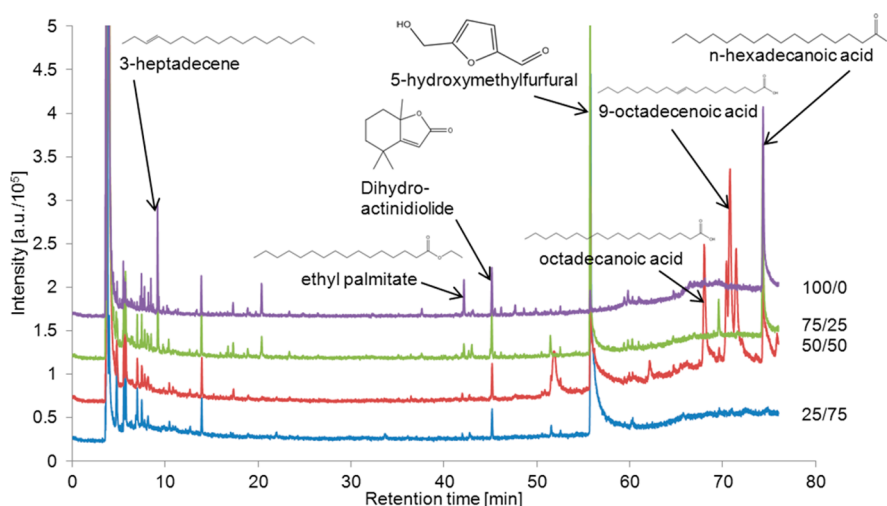
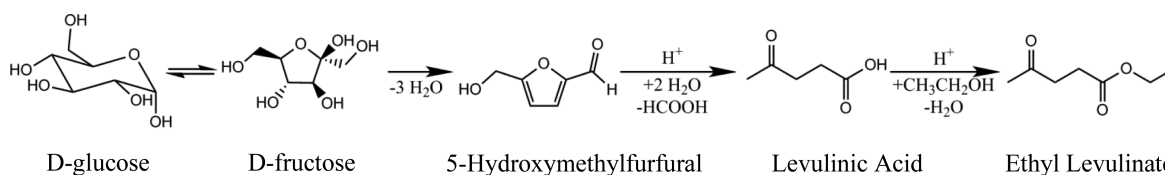


**Figure 2.** Chromatographic analysis of the compounds in the reactor effluent after the mild liquefaction at the ethanol/water ratio of 100/0, 75/25, 50/50, and 25/75 (v/v,  $T = 453$  K,  $p = 14$  to 20 bar depending on the E/W ratio).

### Scheme 1. Reaction Chain of Glucose Dehydration during Liquefaction Using Ethanol As Cosolvent



The product distribution in the liquefaction depended strongly on the applied E/W ratio. With the E/W ratio of 25/75 the main product was 5-HMF, whereas smaller amounts of furfural and acetic acid (not shown) were also identified. The five-membered ring, 5-HMF, is a well-known biomass-based platform compound, which possesses a high potential for being used as renewable feedstock.<sup>32,33</sup> Free fatty acids, e.g. n-hexadecanoic (C16:0) and 9-octadecenoic (C18:1) acid, were also identified in the samples. These fatty acids are related to the carotenogenesis in *Dunaliella salina* during the high light adaptation.<sup>34</sup> We are using in our study the remnant algal biomass cultivated under high light irradiance which is the precondition for carotenogenesis and explains the presence of the fatty acids. This indicates also that hexane does not exhaustively extract all lipids and that the fatty acids were likely hydrolyzed from triglycerides during the liquefaction. Acetic acid was identified in small concentrations and likely works catalytically in the liquefaction, facilitating hydrolysis, dehydration, and esterification.

The influence of the catalyst Nafion NRS0 was investigated using pure ethanol as solvent. Chromatographs including the main identified compounds in the reactor effluent are illustrated in Figure S1. The distribution of the product compounds (as Area-%) are given in Table S2 in the Supporting Information. It was observed that the acidic catalyst promoted ethyl ester formation and that the concentrations of ethyl levulinate and palmitate were clearly higher in the catalyzed experiments than in those without catalyst. The 5-HMF concentration was negligible with pure ethanol as solvent in both experiments. In the presence of the acidic catalyst, it is likely that the 5-HMF is easily further hydrolyzed to levulinic acid and that the ethyl levulinate detected in the catalyzed experiments is the esterified product of the acid. This has been demonstrated in many studies, where the reactivity and decomposition of model

compounds, e.g. fructose and 5-HMF, have been investigated using various catalysts.<sup>35</sup> Under the influence of the acidic zeolite, H-ZSM-5, the decomposition of 5-HMF to levulinic acid was reported using *Chlorococcum sp.* as algal feedstock.<sup>14</sup> However, it should be mentioned here that Nafion as catalyst is likely not an optimal choice for mild liquefaction. The acidic sites inside of the spherical beads are barely accessible for the solid algae cell fragments, leaving only the sites on the outer surface active. The beads swell only moderately in ethanol, further limiting the accessibility of larger molecules on the catalytic active sites.

The identified molecules in the liquefaction effluent (Figure 2) are formed by the hydrolysis of carbohydrates. Initially, the remnant algal biomass contains a high concentration of carbohydrates as storage molecules. The liquefaction likely releases acidic compounds which catalyze the decomposition and dehydration reactions. Scheme 1 illustrates the reaction chain for the dehydration of glucose to 5-HMF. It is known that the dehydration rate is higher for D-fructose than for D-glucose.<sup>36</sup> In the presence of the acidic catalyst or acidic decomposition products, 5-HMF reacts easily to levulinic acid while simultaneously forming formic acid as a side product.<sup>37</sup> During liquefaction with ethanol as the solvent, the levulinic acid is esterified to the ethyl levulinate. Reactions, catalysts, and solvent systems for the conversion of sugars (e.g., glucose and fructose), starch, and cellulose to 5-HMF and levulinic acid have been intensively reported in the literature.<sup>38–40</sup> Our present study demonstrates that the direct conversion of algal remnant biomass to the 5-HMF is possible in one step without prior purification or separation of the carbohydrates contained within the algal remnant. This approach is comparable to that presented by Wang et al., where *Chlorococcum sp.* was converted to 5-HMF in the presence of ZSM-5 zeolite.<sup>14</sup>

**Computational Estimation of the 5-HMF Recovery with MIBK.** The prospect to extract 5-HMF from a mixture of ethanol/water which simulates the reactor effluent was first analyzed computationally. The extraction of the product compounds with a promising solvent is essential, because in the practical applications the reactor effluent contains not only desired chemical products but also water-soluble nutrient residues, salts, partially decomposed proteins, and carbohydrates. The MIBK was selected as the extraction medium because MIBK is reported to be highly efficient for recovering 5-HMF in two-phase systems.<sup>39,41</sup>

The EtOH-H<sub>2</sub>O-MIBK ternary system establishes a liquid–liquid phase equilibrium at 298 K,<sup>28</sup> and the partition of 5-HMF between the two liquid phases was estimated computationally. The solubility of 5-HMF was predicted on four ternary compositions along the binodal curve published by Chafer et al.<sup>28</sup> Figure 3a ( $i = 50$ ) and Figure 3b ( $i = 25$ ) show the ternary phase diagram including the binodal curve at 298 K and the points  $I_{50}^E$  to  $IV_{50}^E$  and  $I_{25}^E$  to  $IV_{25}^E$ , accordingly. The binary ethanol/water mole compositions of 0.236/0.764 and 0.0932/0.9068 (mol/mol) correspond to the E/W ratios of 50/50 (v/v) and 25/75 (v/v), which are as well illustrated in the figures. Tables 2 (E/W 50/50) and Table 3 (E/W 25/75) list the overall compositions of  $I_i^M$  to  $IV_i^M$  (both phases) and the corresponding composition of the MIBK rich phases,  $I_i^E$  to  $IV_i^E$ .

The relative solubility of 5-HMF in the MIBK rich phase and aqueous phases was then estimated for the compositions  $I_i^E$  to  $IV_i^E$  ( $i = 25$  and 50) and the corresponding aqueous phase compositions  $I_i^A$  to  $IV_i^A$  (not shown) using COSMOtherm. With this information the partition of 5-HMF between the phases was obtained. Table 4 and Table 5 list the relative solubility of 5-HMF in the MIBK rich phase at compositions related to the E/W ratios of 50/50 and 25/75, correspondingly. The calculated solubility values are normalized to that at point  $I_{50}^E$  which was the highest estimated solubility obtained in our COSMO-RS calculations. The solubility decreases along the binodal curve (increasing MIBK concentration) so that the relative solubility of 5-HMF at the point  $IV_{50}^E$  is estimated to be only 61.1% of that at  $I_{50}^E$  (see Table 4). This computationally estimated trend was confirmed also experimentally. Figures S2 ( $i = 50$ ) and S3 ( $i = 25$ ) in the Supporting Information illustrate the measured peaks of 5-HMF obtained in the gas chromatographic analysis at points  $I_i^E$  to  $IV_i^E$ . The 5-HMF peak areas in Figures S2 and S3 are in accordance with the relative solubility of 5-HMF estimated by COSMO-RS showing a decreasing concentration of 5-HMF when moving from the point  $I_i^E$  to the point  $IV_i^E$ .

Solubility is not the only factor influencing the recovery of a compound. The phase ratio, i.e. the relative amount of the phases in a two phase system, has to be considered as well. The phase ratio  $K$  is defined as

$$K = \frac{n_E}{n_{AQ}} \quad (3)$$

i.e. the amount ratio of MIBK rich phase in relation to the aqueous phase.

$K$  can be determined graphically by the lever rule from the phase diagram or solved analytically, if the overall and one tie line compositions are known. The phase ratio  $K$  (see Table 4) varies strongly depending on the point considered. For  $I_{50}^E$  the phase ratio  $K$  is 1.3. For the point  $IV_{50}^E$  the amount of the MIBK rich phase is about 4.4 times of that of the aqueous phase. With the information on the relative solubility of 5-HMF in both

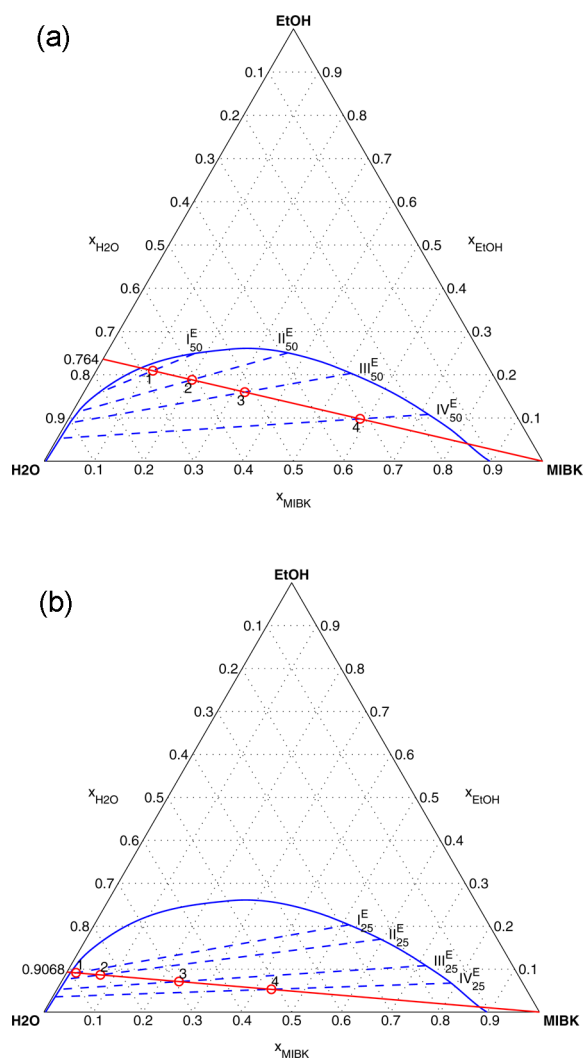


**Figure 3.** a. Phase diagram for the system water–ethanol–MIBK (methyl *tert*-butyl ketone) at 298 K. The points in the figure refer to compositions (1)  $I_{50}^M$ , (2)  $II_{50}^M$ , (3)  $III_{50}^M$ , and (4)  $IV_{50}^M$ . The binodal curve (blue line) and the tie lines (dash line) are taken from Chafer et al.<sup>28</sup> b. Phase diagram for the system water–ethanol–MIBK (methyl *tert*-butyl ketone) at 298 K. The points in the figure refer to compositions (1)  $I_{25}^M$ , (2)  $II_{25}^M$ , (3)  $III_{25}^M$ , and (4)  $IV_{25}^M$ . The binodal curve (blue line) and the tie lines (dash line) are taken from Chafer et al.<sup>28</sup>

**Table 2.** Calculated Mole Fractions  $x_i$  of Ethanol and MIBK Corresponding to the E/W Ratio of 50/50 (v/v)<sup>b</sup>

	$x_i$ before separation <sup>a</sup>		$x_i$ in MIBK rich phase <sup>a</sup>		
	EtOH	MIBK	EtOH	MIBK	
$I_{50}^M$	0.2090	0.1129	$I_{50}^E$	0.2485	0.1768
$II_{50}^M$	0.1880	0.2019	$II_{50}^E$	0.2505	0.3636
$III_{50}^M$	0.1597	0.3220	$III_{50}^E$	0.2032	0.5142
$IV_{50}^M$	0.0980	0.5840	$IV_{50}^E$	0.1082	0.7167

<sup>a</sup> $[H_2O] = 1 - [EtOH] - [MIBK]$ . <sup>b</sup>The mole fractions  $x_i$  in MIBK rich phase are taken from Chafer et al.<sup>28</sup>

phases and the phase ratio  $K$ , the absolute partition of 5-HMF between the phases was calculated. The partition ratio  $\eta$  of 5-HMF is defined as the amount of 5-HMF existing in the MIBK rich phase ( $E$ ) in relation to that in the aqueous phase as expressed with eq 4:

**Table 3.** Calculated Mole Fractions  $x_i$  of Ethanol and MIBK Corresponding to the E/W Ratio of 25/75 (v/v)<sup>b</sup>

	$x_i$ before separation <sup>a</sup>		$x_i$ in MIBK rich phase <sup>a</sup>	
	EtOH	MIBK	EtOH	MIBK
I <sub>25</sub> <sup>M</sup>	0.0938	0.0194	I <sub>25</sub> <sup>E</sup>	0.2032
II <sub>25</sub> <sup>M</sup>	0.0866	0.0708	II <sub>25</sub> <sup>E</sup>	0.1696
III <sub>25</sub> <sup>M</sup>	0.0711	0.2368	III <sub>25</sub> <sup>E</sup>	0.1082
IV <sub>25</sub> <sup>M</sup>	0.0529	0.4328	IV <sub>25</sub> <sup>E</sup>	0.0674

<sup>a</sup>[H<sub>2</sub>O] = 1 - [EtOH] - [MIBK]. <sup>b</sup>The mole fractions  $x_i$  in MIBK rich phase are taken from Cháfer et al.<sup>28</sup>

**Table 4.** Extract Mole Fractions, Relative Solubility, Phase Ratio  $K$ , and the Fraction (%) of 5-HMF in the MIBK Rich Phase Corresponding to the E/W Ratio of 50/50 (v/v)

point on the tie line	relative solubility [w%]	solubility ratio <sup>a</sup>	$K$	5-HMF [%]
I <sub>50</sub> <sup>E</sup>	100.0	2.05	1.301	72.77
II <sub>50</sub> <sup>E</sup>	86.5	3.53	1.183	80.67
III <sub>50</sub> <sup>E</sup>	74.7	4.41	1.639	87.83
IV <sub>50</sub> <sup>E</sup>	61.1	5.77	4.368	96.18

<sup>a</sup>The ratio of 5-HMF solubility between the MIBK rich phase and the corresponding aqueous phase at the end points of the tie lines.

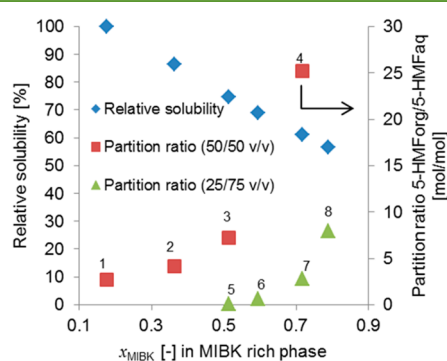
**Table 5.** Extract Mole Fractions, Relative Solubility, Phase Ratio  $K$ , and the Fraction (%) of 5-HMF in the MIBK Rich Phase for Experiments Corresponding to the E/W Ratio of 25/75 (v/v)

point on the tie line	relative solubility [w%] <sup>a</sup>	solubility ratio <sup>b</sup>	$K$	5-HMF [%]
I <sub>25</sub> <sup>E</sup>	74.7	4.41	0.027	10.49
II <sub>25</sub> <sup>E</sup>	68.9	4.83	0.123	37.33
III <sub>25</sub> <sup>E</sup>	61.1	5.77	0.484	73.64
IV <sub>25</sub> <sup>E</sup>	56.5	6.57	1.206	88.79

<sup>a</sup>Relative solubility of 5-HMF normalized to the solubility at point I<sub>50</sub><sup>E</sup> (100%). <sup>b</sup>The ratio of 5-HMF solubility between the MIBK rich phase and the corresponding aqueous phase at the end points of the tie lines.

$$\eta = \frac{RS_E}{RS_A} \cdot K \quad (4)$$

Figure 4 shows the calculated relative solubilities on the compositions I<sub>i</sub><sup>E</sup> to IV<sub>i</sub><sup>E</sup> ( $i = 25$  and 50) along the binodal curve.

**Figure 4.** Relative solubility of 5-HMF as a function of  $x_{\text{MIBK}}$  and the partition ratio of 5-HMF according to COSMO-RS calculations. Index org refers to MIBK rich phase, and aq refers to the aqueous phase. Points in the illustration refer to compositions (1) I<sub>50</sub><sup>E</sup>, (2) II<sub>50</sub><sup>E</sup>, (3) III<sub>50</sub><sup>E</sup>, (4) IV<sub>50</sub><sup>E</sup>, (5) I<sub>25</sub><sup>E</sup>, (6) II<sub>25</sub><sup>E</sup>, (7) III<sub>25</sub><sup>E</sup>, and (8) IV<sub>25</sub><sup>E</sup>.

The solubility decreases steadily along increasing MIBK mole fraction. The partition ratio  $\eta$  on the corresponding composition points is illustrated as well in Figure 4. As seen here, the 5-HMF is highly concentrated in the MIBK rich phase on the composition points I<sub>50</sub><sup>E</sup> to IV<sub>50</sub><sup>E</sup>, e.g. for IV<sub>50</sub><sup>E</sup> the partition ratio  $\eta = 25.2$ . This means that the 5-HMF could be found mainly in the MIBK rich phase, and only a small fraction would be lost in the aqueous phase. The corresponding percentage of 5-HMF recoverable in the MIBK rich phase is presented in Tables 4 and 5. By considering both the solubility estimation by COSMOtherm as well as the phase ratio  $K$ , it was estimated that 96.2% of the formed 5-HMF is recoverable in the MIBK rich phase, and only 3.8% would be lost in the aqueous phase for the point IV<sub>50</sub><sup>E</sup>. For the E/W ratio of 25/75 (v/v) presented in Table 5 the best recovery percentage was 88.9% with the partition ratio  $\eta = 7.92$  for IV<sub>25</sub><sup>E</sup>. Here, the partition of 5-HMF between the phases decreases strongly between the points IV<sub>25</sub><sup>E</sup> to I<sub>25</sub><sup>E</sup>. For I<sub>25</sub><sup>E</sup> only 10.5% of the 5-HMF formed exists in the MIBK rich phase, whereas the majority (89.5%) would remain in the aqueous phase.

**Experimental Validation of 5-HMF Recovery with MIBK.** Finally, the amount of 5-HMF recoverable from the *D. salina* samples in the mild liquefaction using E/W ratios of 50/50 (v/v) and 25/75 (v/v) using MIBK as extraction solvent were quantified experimentally. Various doses of MIBK were directly added to the reactor effluent samples after solid separation. Expectedly, these ternary mixtures separated into aqueous and MIBK rich phases at room temperature according to the phase diagram because the overall compositions were within the miscibility gap. Figure S4 in the Supporting Information illustrates the graphs, and Table S3 lists the main peaks identified in the MIBK rich phase using gas chromatography. 5-HMF was the main compound in the MIBK extract for each of the E/W ratios tested for mild liquefaction. The amount of 5-HMF in the MIBK extract was quantified, and the results are shown in Figures 5a and b. Expectedly, it can be seen that the 5-HMF concentration tends to decrease as a function of the increasing MIBK mole fraction (right axis). In order to determine the amount of HMF recovered experimentally, the 5-HMF in the MIBK rich phase was quantified. The overall yield of 5-HMF increased in line with MIBK concentration in the extract. Quantitatively, 7.1 mg of 5-HMF was obtained per gram *D. salina* remnant (dw) using a liquefaction E/W ratio of 50/50 (v/v) (Figure 5a). When using an E/W ratio of 25/75 (v/v) the amount of 5-HMF recovered was clearly dependent on the amount of MIBK in the extract. Here, up to 10.3 mg of 5-HMF per gram of the remnant (dw) was recovered. In the study of Wang et al. the isolated yield of 5-HMF in relation to monosaccharides present in the *Chlorococcum sp.* algal sample was reported to be 7.5% using an H-ZSM-5 catalyst with 50 g L<sup>-1</sup>.<sup>14</sup> Studies using the sugars fructose and glucose that show a high yield of 5-HMF are weakly comparable to the approach presented in this work, because the separation and purification of the sugars from biomass is typically not considered.

At this stage, the quantitative yields of 5-HMF reported in this study are moderate (~1%). The 5-HMF is only a small fraction of the solubles. However, one should note that the algal biomass contains also nitrogen compounds, other decomposition products of carbohydrates, starch, or monosugars which possible are soluble in the mild liquefaction conditions but were not identified. For comparison, e.g. cyclic and straight amine derivatives, ketone and alcohol derivatives, phenols, and

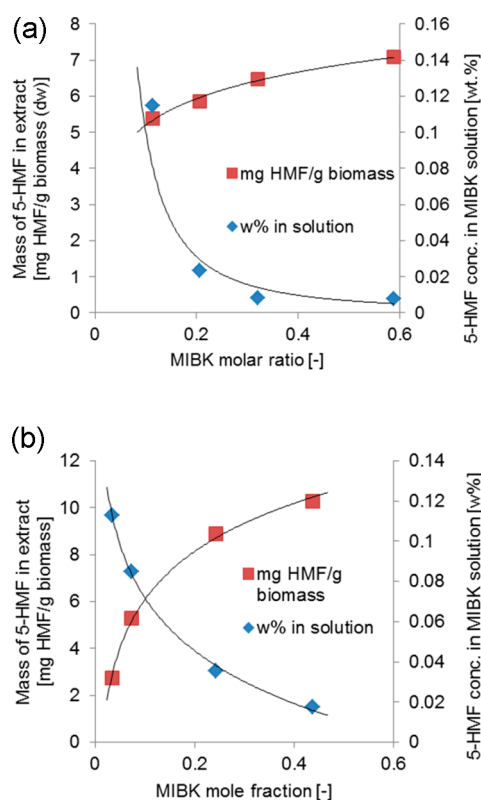


**Figure 5.** a. Concentration of 5-hydroxy methyl furfural in the MIBK rich phase (right axis) and the overall yield of 5-HMF (left axis) in experiment using an ethanol/water ratio of 50/50 (v/v). The MIBK mole fraction ( $x$ -axis) refers to the overall mole fraction before phase separation. b. Concentration of 5-hydroxy methyl furfural in the MIBK rich phase (right axis) and the overall mass yield of 5-HMF (left axis) in experiment using an ethanol/water ratio of 25/75 (v/v). The MIBK mole fraction ( $x$ -axis) refers to the overall mole fraction before phase separation.

esters were reported in the aqueous phase after the conventional, more severe solvolysis liquefaction of *Chlorella pyrenoidosa*.<sup>29</sup> However, the aim of this study was to demonstrate the proof-of-principle for a direct conversion of algal remnant to chemical compounds by mild thermal treatment. The reactor conditions during the liquefaction can be optimized to improve the yields further. The use of other catalysts, e.g. heteropolyacids or zeolites, and the application of multiphase reactor conditions should be investigated. The use of Sn-Beta zeolites would be highly promising as it strongly facilitates the isomerization of glucose to fructose, the initial step in the formation of 5-HMF from starch or cellulose.<sup>42</sup> However, one should note that in view of an integrated biorefinery framework, the approach converting the remnant fraction of algal biomass under mild conditions for chemicals likely could enhance the future commercial prospects of such endeavors.

## CONCLUSIONS

The oil extracted remnant of alga *D. salina* was liquefied in various ethanol/water mixtures at a temperature of 453 K for 60 min. The mild thermal treatment decomposed the remnant cell structure and enabled the identification and separation of the several small sized molecules. The decomposition product 5-HMF formed from algal carbohydrates was found to be one of the products. Furthermore, small concentrations of residual

fatty acids were also detected. A heterogeneous acidic catalyst present in the liquefaction promoted the esterification of the free fatty acids to corresponding ethyl esters.

The proof-of-principle for the direct recovery of 5-HMF from algal remnant was demonstrated in the paper. The 5-HMF was recovered and separated from the aqueous phase by addition of MIBK to initiate phase splitting in several ethanol/water/MIBK mixtures. The solubility of 5-HMF in the ternary mixtures of ethanol/water/MIBK was estimated by the computational method COSMO-RS. Based on the solubility estimation and the known liquid–liquid phase equilibrium of the ternary mixture, the amount of 5-HMF recoverable in the MIBK rich phase could be estimated. Experimentally, 10.3 mg of 5-HMF per gram of the remnant (dw) was recovered in the organic MIBK phase.

## ASSOCIATED CONTENT

### Supporting Information

The Supporting Information is available free of charge on the ACS Publications website at DOI: 10.1021/acssuschemeng.6b01957.

Experimental details and results, i.e. GC/MS graphs for reactor effluent and MIBK rich phase, and identified compounds from the samples in tabular form (PDF)

## AUTHOR INFORMATION

### Corresponding Author

\*Phone: +49 391 6110 318. Fax: +49 391 6110 566. E-mail: rihko@mpi-magdeburg.mpg.de. Corresponding author address: Sandtorstrasse 1, D-39106 Magdeburg, Germany.

### ORCID

Liisa K. Rihko-Struckmann: 0000-0003-0222-7236

### Notes

The authors declare no competing financial interest.

## ACKNOWLEDGMENTS

This research work was partly supported by the Center for Dynamic Systems (CDS) funded by the Federal State Saxony-Anhalt (Germany).

## REFERENCES

- (1) Katz, A. et al. Salinity tolerance and iron Deprivation resistance mechanisms revealed by proteomic analyzes in *Dunaliella Salina*. In *The Alga Dunaliella; Biodiversity, Physiology, Genomics and Biotechnology*; Ben-Amotz, A., Polle, J. E. W., Subba Rao, D. V., Eds.; Science Publishers: Enfield, New Hampshire, USA, 2009.
- (2) Mojaat, M.; Foucault, A.; Pruvost, J.; Legrand, J. Optimal selection of organic solvents for biocompatible extraction of  $\beta$ -carotene from *Dunaliella salina*. *J. Biotechnol.* **2008**, *133*, 433–441.
- (3) Vardon, D. R.; Sharma, B. K.; Blazina, G. V.; Rajagopalan, K.; Strathmann, T. J. Thermochemical conversion of raw and defatted algal biomass via hydrothermal liquefaction and slow pyrolysis. *Bioresour. Technol.* **2012**, *109*, 178–187.
- (4) López Barreiro, D.; Prins, W.; Ronsse, F.; Brilman, W. Hydrothermal liquefaction (HTL) of microalgae for biofuel production: State of the art review and future prospects. *Biomass Bioenergy* **2013**, *53*, 113–127.
- (5) López Barreiro, D.; Samori, C.; Terranella, G.; Hornung, U.; Kruse, A.; Prins, W. Assessing microalgae biorefinery routes for the production of biofuels via hydrothermal liquefaction. *Bioresour. Technol.* **2014**, *174*, 256–265.

- (6) Valdez, P. J.; Tocco, V. J.; Savage, P. E. A general kinetic model for the hydrothermal liquefaction of microalgae. *Bioresour. Technol.* **2014**, *163*, 123–127.
- (7) Saber, M.; Nakhshinie, B.; Yoshikawa, K. A review of production and upgrading of algal bio-oil. *Renewable Sustainable Energy Rev.* **2016**, *58*, 918–930.
- (8) Faeth, J. L.; Savage, P. E. Effects of processing conditions on biocrude yields from fast hydrothermal liquefaction of microalgae. *Bioresour. Technol.* **2016**, *206*, 290–293.
- (9) Lee, A.; Lewis, D.; Kalaitzidis, T.; Ashman, P. Technical issues in the large-scale hydrothermal liquefaction of microalgal biomass to biocrude. *Curr. Opin. Biotechnol.* **2016**, *38*, 85–89.
- (10) Biller, P.; Ross, A. B. Potential yields and properties of oil from the hydrothermal liquefaction of microalgae with different biochemical content. *Bioresour. Technol.* **2011**, *102*, 215–225.
- (11) Garcia Alba, L.; Torri, C.; Samori, C.; van der Spek, J.; Fabbri, D.; Kersten, S. R. A.; Brilman, D. W. F. Hydrothermal treatment (HTT) of microalgae: evaluation of the process as conversion method in an algal biorefinery concept. *Energy Fuels* **2012**, *26*, 642–657.
- (12) Ho, S. H.; Huang, S. W.; Chen, C. Y.; Hasunuma, T.; Kondo, A.; Chang, J. S. Bioethanol production, using carbohydrate-rich microalgal biomass as feedstock. *Bioresour. Technol.* **2013**, *135*, 191–198.
- (13) Pirwitz, K.; Rihko-Struckmann, L. K.; Sundmacher, K. Valorisation of the aqueous phase obtained from hydrothermally treated *Dunaliella salina* remnant biomass. *Bioresour. Technol.* **2016**, *219*, 64–71.
- (14) Wang, J. J.; Tan, Z. C.; Zhu, C. C.; Miao, G.; Kong, L. Z.; Sun, Y. H. One-pot catalytic conversion of microalgae (*Chlorococcum* sp.) into 5-hydroxymethylfurfural over the commercial H-ZSM-5 zeolite. *Green Chem.* **2016**, *18*, 452–460.
- (15) Jin, B.; Duan, P.; Zhang, C.; Xu, Y.; Zhang, L.; Wang, F. Non-catalytic liquefaction of microalgae in sub- and supercritical acetone. *Chem. Eng. J.* **2014**, *254*, 384–392.
- (16) Yuan, X.; Wang, J.; Zeng, G.; Huang, H.; Pei, X.; Li, H.; Liu, Z.; Cong, M. Comparative studies of thermochemical liquefaction characteristics of microalgae using different organic solvents. *Energy* **2011**, *36*, 6406–6412.
- (17) Singh, R.; Bhaskar, T.; Balagurumurthy, B. Effect of solvent on the hydrothermal liquefaction of macro algae *Ulva fasciata*. *Process Saf. Environ. Prot.* **2015**, *93*, 154–160.
- (18) Duan, P.; Jin, B.; Xu, Y.; Yang, Y.; Bai, X.; Wang, F.; Zhang, L.; Miao, J. Thermo-chemical conversion of *Chlorella pyrenoidosa* to liquid biofuels. *Bioresour. Technol.* **2013**, *133*, 197–205.
- (19) Zhang, J.; Zhang, Y. Hydrothermal liquefaction of microalgae in an ethanol-water Co-solvent to produce biocrude oil. *Energy Fuels* **2014**, *28*, 5178–5183.
- (20) Jena, U.; McCurdy, A. T.; Warren, A.; Summers, H.; Ledbetter, R. N.; Hoekman, S. K.; Seefeldt, L. C.; Quinn, J. C. Oleaginous yeast platform for producing biofuels via co-solvent hydrothermal liquefaction. *Biotechnol. Biofuels* **2015**, *8*, 167.
- (21) Klamt, A. Conductor-like Screening Model for Real Solvents: A New Approach to the Quantitative Calculation of Solvation Phenomena. *J. Phys. Chem.* **1995**, *99*, 2224–2235.
- (22) Vasiliu, M.; Guynn, K.; Dixon, D. A. Prediction of the Thermodynamic Properties of Key Products and Intermediates from Biomass. *J. Phys. Chem. C* **2011**, *115*, 15686–15702.
- (23) Hahnenkamp, I.; Graubner, G.; Gmehling, J. Measurement and prediction of solubilities of active pharmaceutical ingredients. *Int. J. Pharm.* **2010**, *388*, 73–81.
- (24) McBride, K.; Gaide, T.; Vorholt, A.; Behr, A.; Sundmacher, K. Thermomorphic solvent selection for homogeneous catalyst recovery based on COSMO-RS. *Chem. Eng. Process.* **2016**, *99*, 97–106.
- (25) Eckert, F.; Klamt, A. *COSMOtherm Version C15*; COSMOlogic GmbH & Co.KG: Leverkusen, Germany, 2015.
- (26) Bligh, E. G.; Dyer, W. J. A rapid method of total lipid extraction and purification. *Can. J. Biochem. Physiol.* **1959**, *37*, 911–917.
- (27) González López, C. V.; García, M. D. C. C.; Fernández, F. G. A.; Bustos, C. S.; Chisti, Y.; Sevilla, J. M. F. Protein measurements of microalgal and cyanobacterial biomass. *Bioresour. Technol.* **2010**, *101*, 7587–7591.
- (28) Cháfer, A.; Lladosa, E.; Montón, J. B.; de la Torre, J. Measurements and correlation of liquid–liquid equilibria of 4-methyl-2-pentanone + ethanol + water and 4-methyl-2-pentanone + n-butanol + water ternary systems between 283.2 and 323.2 K. *Fluid Phase Equilib.* **2012**, *317*, 89–95.
- (29) Peng, X. W.; Ma, X. Q.; Lin, Y. S. Investigation on Characteristics of Liquefied Products from Solvolysis Liquefaction of *Chlorella pyrenoidosa* in Ethanol-Water Systems. *Energy Fuels* **2016**, *30*, 6475–6485.
- (30) Weingarten, R.; Rodriguez-Beuerman, A.; Cao, F.; Luterbacher, J. S.; Alonso, D. M.; Dumesic, J. A.; Huber, G. W. Selective Conversion of Cellulose to Hydroxymethylfurfural in Polar Aprotic Solvents. *ChemCatChem* **2014**, *6*, 2229–2234.
- (31) Wang, T.; Nolte, M. W.; Shanks, B. H. Catalytic dehydration of C-6 carbohydrates for the production of hydroxymethylfurfural (HMF) as a versatile platform chemical. *Green Chem.* **2014**, *16*, 548–572.
- (32) van Putten, R.-J.; van der Waal, J. C.; de Jong, E.; Rasrendra, C. B.; Heeres, H. J.; de Vries, J. G. Hydroxymethylfurfural, A Versatile Platform Chemical Made from Renewable Resources. *Chem. Rev.* **2013**, *113*, 1499–1597.
- (33) Rosatella, A. A.; Simeonov, S. P.; Frade, R. F. M.; Afonso, C. A. M. 5-Hydroxymethylfurfural (HMF) as a building block platform: Biological properties, synthesis and synthetic applications. *Green Chem.* **2011**, *13*, 754–793.
- (34) Mendoza, H.; Martel, A.; Jiménez del Rio, M.; García Reina, G. Oleic acid is the main fatty acid related with carotenogenesis in *Dunaliella salina*. *J. Appl. Phycol.* **1999**, *11*, 15–19.
- (35) Fachri, B. A.; Abdilla, R. M.; van de Bovenkamp, H. H.; Rasrendra, C. B.; Heeres, H. J. Experimental and Kinetic Modeling Studies on the Sulfuric Acid Catalyzed Conversion of D-Fructose to 5-Hydroxymethylfurfural and Levulinic Acid in Water. *ACS Sustainable Chem. Eng.* **2015**, *3*, 3024–3034.
- (36) Huang, H.; Denard, C. A.; Alamillo, R.; Crisci, A. J.; Miao, Y.; Dumesic, J. A.; Scott, S. L.; Zhao, H. Tandem Catalytic Conversion of Glucose to 5-Hydroxymethylfurfural with an Immobilized Enzyme and a Solid Acid. *ACS Catal.* **2014**, *4*, 2165–2168.
- (37) Weingarten, R.; Conner, W. C., Jr.; Huber, G. W. Production of levulinic acid from cellulose by hydrothermal decomposition combined with aqueous phase dehydration with a solid acid catalyst. *Energy Environ. Sci.* **2012**, *5*, 7559–7574.
- (38) Caes, B. R.; Teixeira, R. E.; Knapp, K. G.; Raines, R. T. Biomass to Furanics: Renewable Routes to Chemicals and Fuels. *ACS Sustainable Chem. Eng.* **2015**, *3*, 2591–2605.
- (39) Jimenez-Morales, I.; Moreno-Recio, M.; Santamaria-Gonzalez, J.; Maireles-Torres, P.; Jimenez-Lopez, A. Mesoporous tantalum oxide as catalyst for dehydration of glucose to 5-hydroxymethylfurfural. *Appl. Catal., B* **2014**, *154–155*, 190–196.
- (40) Weingarten, R.; Cho, J.; Xing, R.; Conner, W. C., Jr.; Huber, G. W. Kinetics and Reaction Engineering of Levulinic Acid Production from Aqueous Glucose Solutions. *ChemSusChem* **2012**, *5*, 1280–1290.
- (41) Roman-Leshkov, Y.; Chheda, J. N.; Dumesic, J. A. Phase modifiers promote efficient production of hydroxymethylfurfural from fructose. *Science* **2006**, *312*, 1933–1937.
- (42) Nikolla, E.; Roman-Leshkov, Y.; Moliner, M.; Davis, M. E. "One-Pot" Synthesis of 5-(Hydroxymethyl)furfural from Carbohydrates using Tin-Beta Zeolite. *ACS Catal.* **2011**, *1*, 408–410.